

## Crystal and Molecular Structure of the Anion $[\text{Rh}_7(\text{CO})_{16}]^{3-}$ in Its Tetramethylammonium Salt †

Vincenzo G. Albano

*Dipartimento di Chimica 'G. Ciamician' dell'Università, Via F. Selmi 2, 40126 Bologna, Italy*

Pier L. Bellon and Gianfranco Ciani\*

*Istituto di Chimica Strutturistica Inorganica, Via G. Venezian 21, 20133 Milano, Italy*

The structure of  $[\text{NMe}_4]_3[\text{Rh}_7(\text{CO})_{16}]$  has been reinvestigated by diffractometric X-ray analysis. The crystals are orthorhombic, space group  $Pnma$ , with  $a = 24.537(5)$ ,  $b = 13.933(3)$ ,  $c = 12.218(4)$  Å, and  $Z = 4$ . The refinements were carried out by full-matrix least squares, on the basis of 2 411 independent significant reflections, to a final  $R$  value of 0.026. The  $\text{Rh}_7$  cluster is a monocapped octahedron and the ligand geometry exhibits some distortions with respect to the ideal  $C_{3v}$  symmetry. The Rh–Rh bond lengths are in the range 2.711(1)–2.880(1) Å. The capping metal is bound to the octahedron with one longer and two shorter metal–metal bonds (difference of 0.14 Å). The three  $\mu_3$ -CO ligands show asymmetric bonding, in agreement with the results of  $^{13}\text{C}$  n.m.r. investigations.

In 1969 we reported the structural characterization of the  $[\text{Rh}_7(\text{CO})_{16}]^{3-}$  anion, synthesized by Martinengo and Chini,<sup>1</sup> which was the first example of a monocapped octahedral metallic cluster and, at that time, the first compact cluster species with more than six metal atoms.<sup>2</sup> In the following years the anion was studied from the point of view of its reactivity,<sup>3</sup> and its behaviour in solution, by  $^{13}\text{C}$  n.m.r. spectroscopy.<sup>4</sup> Moreover it was employed as a starting compound for the synthesis of larger clusters, such as  $[\text{Rh}_{11}(\text{CO})_{23}]^{3-}$  (ref. 5) and  $[\text{Rh}_{14}(\text{CO})_{25}]^{4-}$  (ref. 6), and of clusters containing interstitial heteroatoms, such as  $[\text{Rh}_6\text{N}(\text{CO})_{15}]^-$ .<sup>7</sup> The structure, obtained then by photographic methods, was of a quality nowadays regarded as unsatisfactory. We have, therefore, decided to undertake a more accurate single-crystal X-ray analysis of the anion in the same salt  $[\text{NMe}_4]_3[\text{Rh}_7(\text{CO})_{16}]$  in order to obtain better structural parameters. The results are reported here and discussed in comparison with the structures of other monocapped octahedral clusters characterized more recently and in the light of the  $^{13}\text{C}$  n.m.r. results.

### Results and Discussion

The anion is illustrated in the Figure and bond distances are given in Table 1. It lies on a crystallographic mirror plane passing through Rh(2), Rh(4), and Rh(5). The overall idealized symmetry is  $C_{3v}$  but significant distortions, present both in the metallic monocapped octahedral skeleton [especially the displacement of the capping Rh(5) from the  $C_3$  axis] and in the ligand geometry, reduce it (at least in the solid state) to the crystallographically imposed  $C_s$  symmetry.

The Rh–Rh bond lengths are in the range 2.711(1)–2.880(1) Å, with an overall mean of 2.774 Å. From a more detailed analysis, based on the idealized  $C_{3v}$  symmetry, the metal–metal bonds can be assigned to four different classes: (i) basal non-capped triangle (3), mean 2.730 Å; (ii) interlayer edges connecting the basal and the central triangle (6), mean 2.781 Å; (iii) central triangle (3), mean 2.792 Å; (iv) distances involving the Rh(5) capping atom (3), mean 2.785 Å. The cap, however, is

significantly asymmetric, with one longer [2.880(1) Å] and two shorter bonds [2.738(1) Å]. The longest Rh–Rh bonds are associated with the metals of the central triangle, which exhibit the greatest metal–metal connectivity (5). The shortest distances, on the other hand, are found in the basal triangle, whose edges are spanned by bridging CO ligands, which are known to add extra stabilization to metal–metal interactions.

Seven of the 16 CO ligands are terminally bonded, one per metal atom, with mean Rh–C and C–O bond lengths of 1.860 and 1.140 Å, respectively. Six CO groups doubly bridge the edges of the basal triangle (almost symmetric) and the edges of the cap (moderately asymmetric), with overall mean Rh–C and C–O bond lengths of 2.039 and 1.166 Å, respectively. Three CO groups triply bridge faces Rh(1,3,4), Rh(1',3',4), and Rh(2,3,3') and are markedly asymmetric: those on the

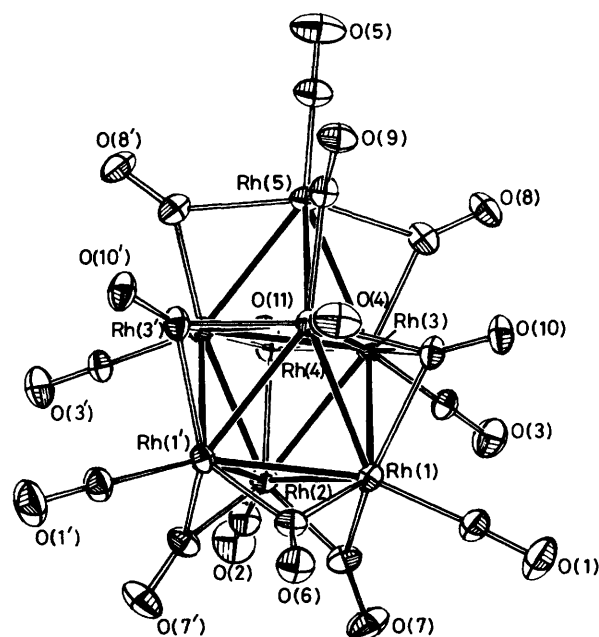


Figure. A view of the anion  $[\text{Rh}_7(\text{CO})_{16}]^{3-}$ . A crystallographic mirror plane passes through the Rh(2), Rh(4), and Rh(5) atoms. The carbonyl groups are indicated by the numbers of their oxygen atoms

† Tris(tetramethylammonium) hexa- $\mu$ -carbonyl-tri- $\mu_3$ -carbonyl-cyclo-hepta(carbonylrhodate) (15Rh–Rh).

Supplementary data available: see Instructions for Authors, *J. Chem. Soc., Dalton Trans.*, 1988, Issue 1, pp. xvii–xx.

**Table 1.** Bond distances (Å) and angles (°) within  $[\text{NMe}_4]_3[\text{Rh}_7(\text{CO})_{16}]^a$ 

Anion							
Rh(1)–Rh(1')	2.711(1)	Rh(1)–C(1)	1.856(7) [1.830(9)] <sup>b</sup>	Rh(5)–C(8)	2.122(8) [2.094(8)]		
Rh(1)–Rh(2)	2.740(1)	Rh(2)–C(2)	1.892(10) [1.845(12)]	Rh(4)–C(9)	2.119(10) [2.101(11)]		
Rh(1)–Rh(3)	2.757(1)	Rh(3)–C(3)	1.859(7) [1.836(8)]	Rh(5)–C(9)	2.013(9) [1.994(10)]		
Rh(1)–Rh(4)	2.798(1)	Rh(4)–C(4)	1.854(9) [1.833(10)]	Rh(1)–C(10)	2.264(7) [2.239(7)]		
Rh(2)–Rh(3)	2.788(1)	Rh(5)–C(5)	1.843(12) [1.803(14)]	Rh(3)–C(10)	2.294(6) [2.281(7)]		
Rh(3)–Rh(3')	2.765(1)	Rh(1)–C(6)	2.013(7) [2.002(8)]	Rh(4)–C(10)	2.091(6) [2.072(8)]		
Rh(3)–Rh(4)	2.805(1)	Rh(1)–C(7)	2.018(7) [2.000(8)]	Rh(2)–C(11)	2.427(9) [2.403(10)]		
Rh(3)–Rh(5)	2.738(1)	Rh(2)–C(7)	1.975(7) [1.953(8)]	Rh(3)–C(11)	2.110(7) [2.098(7)]		
Rh(4)–Rh(5)	2.880(1)	Rh(3)–C(8)	2.042(7) [2.036(8)]				
				Cations			
C(1)–O(1)	1.158(8) [1.180(10)]	C(7)–O(7)	1.176(7) [1.202(9)]	N(1)–C(N11)	1.506(9)		
C(2)–O(2)	1.119(11) [1.156(14)]	C(8)–O(8)	1.155(8) [1.189(9)]	N(1)–C(N12)	1.483(10)		
C(3)–O(3)	1.137(7) [1.150(9)]	C(9)–O(9)	1.162(10) [1.188(12)]	N(1)–C(N13)	1.503(10)		
C(4)–O(4)	1.132(10) [1.160(12)]	C(10)–O(10)	1.164(7) [1.195(8)]	N(1)–C(N14)	1.508(9)		
C(5)–O(5)	1.136(12) [1.153(15)]	C(11)–O(11)	1.184(9) [1.210(11)]	N(2)–C(N21)	1.505(12)		
C(6)–O(6)	1.171(10) [1.186(12)]			N(2)–C(N22)	1.364(17)		
				N(2)–C(N23)	1.457(19)		
Rh(1')–Rh(1)–C(1)	153.8(2)	Rh(3)–Rh(5)–C(5)	141.7(2)	Rh(2)–C(2)–O(2)	180.8(8)	Rh(3)–C(10)–O(10)	130.9(5)
Rh(2)–Rh(1)–C(1)	133.1(2)	Rh(4)–Rh(5)–C(5)	150.2(3)	Rh(3)–C(3)–O(3)	179.0(7)	Rh(4)–C(10)–O(10)	137.3(5)
Rh(3)–Rh(1)–C(1)	115.6(2)	C(1)–Rh(1)–C(6)	106.4(3)	Rh(4)–C(4)–O(4)	179.6(9)	Rh(2)–C(11)–O(11)	128.9(7)
Rh(4)–Rh(1)–C(1)	129.0(2)	C(1)–Rh(1)–C(7)	91.2(3)	Rh(5)–C(5)–O(5)	177.9(11)	Rh(3)–C(11)–O(11)	135.4(3)
Rh(1)–Rh(2)–C(2)	146.7(2)	C(6)–Rh(1)–C(7)	97.3(3)	Rh(1)–C(6)–O(6)	137.6(2)	Rh(1)–C(6)–Rh(1')	84.6(4)
Rh(3)–Rh(2)–C(2)	120.6(3)	C(2)–Rh(2)–C(7)	102.3(3)	Rh(1)–C(7)–O(7)	135.7(6)	Rh(1)–C(7)–Rh(2)	86.7(3)
Rh(1)–Rh(3)–C(3)	88.4(2)	C(7)–Rh(2)–C(7')	83.7(4)	Rh(2)–C(7)–O(7)	137.6(6)	Rh(3)–C(8)–Rh(5)	82.2(3)
Rh(2)–Rh(3)–C(3)	87.6(2)	C(3)–Rh(3)–C(8)	98.2(3)	Rh(3)–C(8)–O(8)	139.8(6)	Rh(4)–C(9)–Rh(5)	88.3(4)
Rh(3')–Rh(3)–C(3)	143.3(2)	C(4)–Rh(4)–C(9)	89.9(4)	Rh(5)–C(8)–O(8)	138.0(6)	Rh(1)–C(10)–Rh(3)	74.4(2)
Rh(4)–Rh(3)–C(3)	143.9(2)	C(5)–Rh(5)–C(8)	98.2(2)	Rh(4)–C(9)–O(9)	136.0(7)	Rh(1)–C(10)–Rh(4)	79.9(2)
Rh(5)–Rh(3)–C(3)	145.3(2)	C(5)–Rh(5)–C(9)	102.8(4)	Rh(5)–C(9)–O(9)	135.7(8)	Rh(3)–C(10)–Rh(4)	79.4(2)
Rh(1)–Rh(4)–C(4)	103.3(3)	Rh(1)–C(1)–O(1)	173.6(7)	Rh(1)–C(10)–O(10)	131.5(5)	Rh(2)–C(11)–Rh(3)	75.5(3)
Rh(3)–Rh(4)–C(4)	149.9(1)					Rh(3)–C(11)–Rh(3')	81.9(3)
Rh(5)–Rh(4)–C(4)	134.2(3)						

<sup>a</sup> Primed atoms are related to unprimed ones by the crystallographic mirror plane. <sup>b</sup> Results of isotropic refinements are given in square brackets.

**Table 2.** Comparison of the metal–metal bond distances (Å) in monocapped octahedral clusters

Compound	M–M Range	Mean M–M for classes*				Ref.
		(i)	(ii)	(iii)	(iv)	
$[\text{Re}_7\text{C}(\text{CO})_{21}]^{3-}$	2.917–3.086(1)	3.080	2.997	2.955	2.929	10
$[\text{Os}_7(\text{CO})_{21}]$	2.806–2.935(6)	2.902	2.857	2.835	2.819	8
$[\text{Rh}_7(\text{CO})_{16}]^{3-}$	2.711–2.880(1)	2.730	2.781	2.792	2.785	This work
$[\text{Rh}_7(\mu\text{-I})(\text{CO})_{16}]^{2-}$	2.740–3.000(5)	2.741	2.786	2.768	2.926	14
$[\text{NiRh}_6(\text{CO})_{16}]^{2-}$	2.707–2.798(5)	2.716	2.782	2.761	2.643	12
	(Rh–Rh)				(Ni–Rh)	
$[\text{Ir}_7(\text{CO})_{12}(\text{C}_8\text{H}_{12})(\text{C}_8\text{H}_{11})(\text{C}_8\text{H}_{10})]$	2.665–2.979(2)	2.781	2.729	2.793	2.781	9
$[\text{Pd}_7(\text{CO})_7(\text{PMe}_3)_7]$	2.729–3.180(5)	2.756	2.798	2.809	2.879	11

\* According to an idealized  $C_{3v}$  cluster symmetry (see text): (i) in the basal triangle; (ii) connecting the basal and the central triangle; (iii) in the central triangle; (iv) within the cap.

two former faces, which are equivalent by symmetry, exhibit one shorter [Rh(4)–C 2.091(6) Å] and two longer [mean Rh(1,3)–C 2.279 Å] bonds, while the third ligand shows one quite longer [Rh(2)–C 2.427(9) Å] and two shorter [Rh(3,3')–C 2.110(7) Å] bonds.

After our previous report<sup>2</sup> of the structure of the anion  $[\text{Rh}_7(\text{CO})_{16}]^{3-}$  some other carbonyl clusters with the same type of metallic array were described, e.g.  $[\text{Os}_7(\text{CO})_{21}]$ ,<sup>8</sup>  $[\text{Ir}_7(\text{CO})_{12}(\text{C}_8\text{H}_{12})(\text{C}_8\text{H}_{11})(\text{C}_8\text{H}_{10})]$ ,<sup>9</sup>  $[\text{Re}_7\text{C}(\text{CO})_{21}]^{3-}$ ,<sup>10</sup>  $[\text{Pd}_7(\text{CO})_7(\text{PMe}_3)_7]$ ,<sup>11</sup> and the mixed-metal cluster  $[\text{NiRh}_6(\text{CO})_{16}]^{2-}$ .<sup>12</sup> All these species are isoelectronic with  $[\text{Rh}_7(\text{CO})_{16}]^{3-}$ , possessing 98 cluster valence electrons, in

accord with various cluster electron-counting theories.<sup>13</sup> Another monocapped octahedral species can be obtained by reaction of  $[\text{Rh}_7(\text{CO})_{16}]^{3-}$  with  $\text{I}_2$ ,<sup>3</sup> namely the anion  $[\text{Rh}_7\text{I}(\text{CO})_{16}]^{2-}$ , containing a bridging iodine ligand on an edge of the cap which causes a rearrangement of the disposition of the CO ligands.<sup>14</sup>

The metal–metal bonding parameters within these species are compared in Table 2. Quite different patterns can be observed: the  $\text{Re}_7$  and the  $\text{Os}_7$  species, containing only terminal carbonyls, show a very similar distribution, with a decrease in length of the metal–metal bonds on passing from the basal triangle to the cap. On the contrary, in the three rhodium-

Table 3. Final positional parameters

Atom	x	y	z	Atom	x	y	z
Rh(1)	0.302 74(2)	-0.152 72(4)	0.121 01(4)	O(7)	0.325 8(3)	-0.116 6(4)	-0.114 5(4)
Rh(2)	0.387 62(3)	-0.250	0.026 41(6)	C(8)	0.430 9(3)	-0.102 4(5)	0.369 7(6)
Rh(3)	0.403 16(2)	-0.150 76(3)	0.222 12(4)	O(8)	0.443 7(2)	-0.031 5(4)	0.411 7(4)
Rh(4)	0.316 35(3)	-0.250	0.319 52(6)	C(9)	0.350 0(4)	-0.250	0.479 2(8)
Rh(5)	0.424 60(3)	-0.250	0.410 65(6)	O(9)	0.332 9(3)	-0.250	0.568 0(5)
C(1)	0.271 8(3)	-0.033 2(5)	0.095 4(6)	C(10)	0.321 2(3)	-0.102 0(5)	0.293 1(6)
O(1)	0.256 3(3)	0.042 5(4)	0.071 9(6)	O(10)	0.309 1(2)	-0.032 1(3)	0.339 6(4)
C(2)	0.442 2(4)	-0.250	-0.083 0(9)	C(11)	0.460 5(4)	-0.250	0.160 7(8)
O(2)	0.474 5(4)	-0.250	-0.147 7(7)	O(11)	0.508 2(3)	-0.250	0.146 3(6)
C(3)	0.421 0(3)	-0.043 8(5)	0.138 5(6)	N(1)	0.401 7(2)	0.041 9(4)	-0.290 3(5)
O(3)	0.432 7(3)	0.021 1(4)	0.087 2(5)	C(N11)	0.072 2(3)	-0.112 6(6)	0.132 6(7)
C(4)	0.246 8(4)	-0.250	0.379 0(8)	C(N12)	0.371 3(5)	-0.031 6(8)	-0.353 6(8)
O(4)	0.204 5(3)	-0.250	0.415 8(6)	C(N13)	0.445 5(4)	-0.004 6(8)	-0.223(1)
C(5)	0.470 2(5)	-0.250	0.530 5(9)	C(N14)	0.364 7(4)	0.096 1(7)	-0.213 5(8)
O(5)	0.499 7(4)	-0.250	0.602 2(8)	N(2)	0.158 8(4)	-0.250	-0.248 4(8)
C(6)	0.243 4(4)	-0.250	0.095 4(8)	C(N21)	0.363 4(7)	0.167 4(8)	0.317(1)
O(6)	0.196 4(3)	-0.250	0.079 0(7)	C(N22)	0.139(1)	-0.250	0.648(1)
C(7)	0.334 9(3)	-0.155 4(5)	-0.031 0(6)	C(N23)	0.217 8(7)	-0.250	-0.235(2)

containing species and in the Pd<sub>7</sub> cluster, which possess bridging CO groups with similar dispositions, the shortest metal-metal bonds are associated with the basal triangle.

In the anion [Rh<sub>7</sub>I(CO)<sub>16</sub>]<sup>2-</sup> (100 cluster valence electrons) the two extra electrons are assumed to occupy a low-lying antibonding orbital delocalized in the cap region, giving rise to a significant lengthening of the metal-metal bonds in this moiety with respect to the parent anion (mean 2.926 vs. 2.785 Å).

A feature observed in some of these clusters is the asymmetric bonding (with two shorter and one longer interactions) of the capping metal. This is the case within the Rh<sub>7</sub> (as mentioned above, difference 0.14 Å) and the Rh<sub>7</sub>I (difference 0.11 Å) anions and, more markedly, within the Ir<sub>7</sub> (difference 0.30 Å) and Pd<sub>7</sub> (difference 0.45 Å) species. Moreover, an octahedral Ru<sub>6</sub> species capped by a gold atom, *i.e.* [Ru<sub>6</sub>C(CO)<sub>15</sub>(NO){Au(PPh<sub>3</sub>)}]<sup>15</sup> shows asymmetric bonding of the above type for the Au atom (difference 0.38 Å). We think that intramolecular factors, such as uneven charge distribution among the metal atoms or intra-ligand steric repulsions, may be largely responsible for the cap asymmetry (especially in the Ir<sub>7</sub> and Rh<sub>7</sub>I species). Also, intermolecular packing contacts can play a significant role, as one can infer on comparing the structures of the strictly related distorted [Rh<sub>7</sub>(CO)<sub>16</sub>]<sup>3-</sup> and undistorted [NiRh<sub>6</sub>(CO)<sub>16</sub>]<sup>2-</sup> anions.

The behaviour of [Rh<sub>7</sub>(CO)<sub>16</sub>]<sup>3-</sup> in solution has been elucidated by <sup>13</sup>C n.m.r. studies.<sup>4</sup> At low temperatures the spectra are fully consistent with the solid-state structure (of idealized C<sub>3v</sub> symmetry). At room temperature a partial scrambling process occurs involving the three terminal and the three edge-bridging groups of the basal triangle. This edge-terminal intra-exchange may be favoured by the low ligand crowding within this moiety. In the derivative [Rh<sub>7</sub>I(CO)<sub>16</sub>]<sup>2-</sup>, due to the presence of the additional iodine ligand on a cap edge, one CO group migrates onto the basal triangle, which then bears a triply bridging ligand in addition to two terminal ligands for each metal. No indication of the exchange process can be deduced by simple inspection of the thermal ellipsoids of the implied CO groups; however the situation of the anion in solution at room temperature must be significantly different from that in the solid state.

An interesting feature of the <sup>13</sup>C n.m.r. investigation [ref. 4(b)] is the prediction of asymmetric bonding for the triply bridging carbonyls, confirmed by the present X-ray analysis. The values of the Rh-CO coupling constants are also in

agreement with the presence of shorter Rh-C bonds for the rhodium atoms of the central triangle [overall mean Rh(central)-C 2.165 Å vs. Rh(basal)-C 2.318 Å]. The same type of asymmetry of the μ<sub>3</sub>-CO groups is present in the isostructural mixed-metal cluster [NiRh<sub>6</sub>(CO)<sub>16</sub>]<sup>2-</sup> (mean 2.14 vs. 2.28 Å).

### Experimental

**Crystal Data.**—C<sub>28</sub>H<sub>36</sub>N<sub>3</sub>O<sub>16</sub>Rh<sub>7</sub>, *M* = 1390.9, orthorhombic, space group *Pnma* (no. 62), *a* = 24.537(5), *b* = 13.933(3), *c* = 12.218(4) Å, *U* = 4 177.0 Å<sup>3</sup>, *Z* = 4, *D*<sub>c</sub> = 2.212 g cm<sup>-3</sup>, *F*(000) = 2 672, Mo-K<sub>α</sub> radiation (λ = 0.710 73 Å), μ(Mo-K<sub>α</sub>) = 27.23 cm<sup>-1</sup>.

**Intensity Measurements.**—A crystal of dimensions 0.12 × 0.14 × 0.28 mm was mounted on a glass fibre in the air. The intensities were collected on an Enraf-Nonius CAD4 automatic diffractometer, using graphite-monochromatized Mo-K<sub>α</sub> radiation. The setting angles of 25 random intense reflections (16 < 2θ < 25°) were used to determine by least-squares fit accurate cell constants and the orientation matrix. The data collection was performed by the ω-scan method, within the limits 3 < θ < 26°. A variable scan speed (from 2 to 20° min<sup>-1</sup>) and a variable scan range of (1 + 0.35tanθ)° were used, with a 25% extension at each end of the scan range for background determination. The total number of reflections measured was 4 558. Three standard intense reflections, monitored every 3 h, revealed no crystal decay. The intensities were corrected for Lorentz and polarization effects. An empirical absorption correction was applied to the data set, based on ψ scans (ψ 0—360° every 10°) of suitable reflections with χ values close to 90°; the relative transmission factors had values in the range 1.00—0.90. 2 411 Independent significant reflections, with *I* > 3σ(*I*), were used in the structure solution and refinements.

**Structure Solution and Refinements.**—All computations were performed on a PDP 11/34 computer, using the Enraf-Nonius structure determination package and the physical constants tabulated therein.

The previously determined<sup>2</sup> positional parameters of the rhodium atoms were used and refined. A successive Fourier difference map showed the locations of all the non-hydrogen

atoms. The anion lies on a crystallographic mirror plane containing Rh(2), Rh(4), and Rh(5); one of the cations also lies on a mirror plane.

The refinements were carried out by full-matrix least squares. At first the thermal motion of the light atoms was treated isotropically and the structure model converged to values of the agreement indices  $R$  and  $R'$  of 0.035 and 0.046, respectively. In the final stages anisotropic thermal factors were assigned to all atoms.\* The hydrogen atoms of the cations were neglected.

The final Fourier difference maps were rather flat showing residual peaks not exceeding  $ca. 1 e \text{ \AA}^{-3}$ . Weights were assigned according to  $w = 4F_o^2/\sigma(F_o^2)^2$ , where  $\sigma(F_o^2) = [\sigma(I)^2 + (pI)^2]^{1/2}/L_p$  ( $I$  and  $L_p$  being the integrated intensity and the Lorentz-polarization correction, respectively);  $p$  was optimized to 0.04. The final values of the agreement indices  $R$  and  $R'$  were 0.026 and 0.035, respectively; the error in an observation of unit weight was 1.211. The final positional parameters are given in Table 3.

### Acknowledgements

We thank the Centro C.N.R. Sintesi e Struttura Composti dei Metalli di Transizione nei Bassi Stati di Ossidazione for financial support and Dr. A. Fumagalli for a gift of the crystal sample.

\* In a recent communication<sup>16</sup> the 'sliding' effect for carbon leading to longer M-C and shorter C-O bond distances in anisotropic *vs.* isotropic refinements of the thermal motion for the carbonyl ligands (as can be seen in Table 1) has been analysed, but not rationalized. In our opinion the effect originates from two major co-operative factors, *i.e.* bond formation and thermal motion. Considering linear M-C-O groups, the former factor causes deformation of the atomic spherical electron density along the M-C-O axis, while thermal spreading is more pronounced orthogonally to the bond axis. The asphericity of the bond deformation is more unbalanced around the carbon than the oxygen atom because of their different electronegativities and is enhanced by the metal-ligand interactions. In isotropic refinements the spherically averaged thermal motion is overestimated along the M-C-O direction with an oversmearing of electron density along the bonds. This artifice compensates for the bond deformation in the electron-rich C-O region but more than compensates for the more diffuse electron density in the M-C region, thus placing the carbon atom nearer to the metal.

### References

- 1 S. Martinengo and P. Chini, *Gazz. Chim. Ital.*, 1972, **102**, 344.
- 2 V. G. Albano, P. L. Bellon, and G. Ciani, *Chem. Commun.*, 1969, 1024.
- 3 S. Martinengo, P. Chini, G. Giordano, A. Ceriotti, V. G. Albano, and G. Ciani, *J. Organomet. Chem.*, 1975, **88**, 375.
- 4 (a) B. T. Heaton, A. D. C. Towl, P. Chini, A. Fumagalli, D. J. A. McCaffrey, and S. Martinengo, *J. Chem. Soc., Chem. Commun.*, 1975, 523; (b) C. Brown, B. T. Heaton, L. Longhetti, D. O. Smith, P. Chini, and S. Martinengo, *J. Organomet. Chem.*, 1979, **169**, 309.
- 5 A. Fumagalli, S. Martinengo, G. Ciani, and A. Sironi, *J. Chem. Soc., Chem. Commun.*, 1983, 453.
- 6 J. L. Vidal and R. C. Schoening, *J. Organomet. Chem.*, 1981, **218**, 217.
- 7 S. Martinengo, G. Ciani, A. Sironi, B. T. Heaton, and J. Mason, *J. Am. Chem. Soc.*, 1980, **101**, 7095.
- 8 C. R. Eady, B. F. G. Johnson, J. Lewis, R. Mason, P. B. Hitchcock, and K. M. Thomas, *J. Chem. Soc., Chem. Commun.*, 1977, 385.
- 9 C. G. Pierpont, *Inorg. Chem.*, 1979, **18**, 2972.
- 10 G. Ciani, G. D'Alfonso, M. Freni, P. Romiti, and A. Sironi, *J. Chem. Soc., Chem. Commun.*, 1982, 339.
- 11 R. Goddard, P. W. Jolly, C. Kruger, K.-P. Schick, and G. Wilke, *Organometallics*, 1982, **1**, 1709.
- 12 A. Fumagalli, G. Longoni, P. Chini, A. Albinati, and S. Bruckner, *J. Organomet. Chem.*, 1980, **202**, 329.
- 13 K. J. Wade, *Chem. Commun.*, 1971, 792; *Adv. Inorg. Chem. Radiochem.*, 1976, **18**, 1; D. M. P. Mingos, *Nature (London), Phys. Sci.*, 1972, **236**, 99; R. Mason and D. M. P. Mingos, *MTP Int. Rev. Sci. Phys. Chem., Ser. 2*, 1975, **11**, 121; J. W. Lauher, *J. Am. Chem. Soc.*, 1978, **100**, 5305; B. K. Teo, *Inorg. Chem.*, 1984, **23**, 1251.
- 14 V. G. Albano, G. Ciani, S. Martinengo, P. Chini, and G. Giordano, *J. Organomet. Chem.*, 1975, **88**, 381.
- 15 B. F. G. Johnson, J. Lewis, W. J. H. Nelson, J. Puga, P. R. Raithby, D. Braga, M. McPartlin, and W. Clegg, *J. Organomet. Chem.*, 1983, **243**, C13.
- 16 D. Braga and T. F. Koetzle, *J. Chem. Soc., Chem. Commun.*, 1987, 144.

Received 22nd May 1987; Paper 7/920